Rotational Echoes as a Tool for Investigating Ultrafast Collisional Dynamics of Molecules

H. Zhang,[1] B. Lavorel,[1] F. Billard,[1] J.-M. Hartmann,[2] E. Hertz,[1] and O. Faucher[1,*]

[1]*Laboratoire Interdisciplinaire CARNOT de Bourgogne, UMR 6303 CNRS-Université de Bourgogne Franche-Comté,*
BP 47870, 21078 Dijon, France
[2]*Laboratoire de Météorologie Dynamique/IPSL, CNRS, École polytechnique, Sorbonne Université,*
École Normale Supérieure, PSL Research University, F-91120 Palaiseau, France

Junyang Ma[1,3] and Jian Wu[3,†]

[3]*State Key Laboratory of Precision Spectroscopy, East China Normal University, Shanghai 200062, China*

Erez Gershnabel,[4] Yehiam Prior,[3,4] and Ilya Sh. Averbukh[4,‡]

[4]*AMOS and Department of Chemical and Biological Physics, The Weizmann Institute of Science, Rehovot 76100, Israel*

We show that recently discovered rotational echoes of molecules provide an efficient tool for studying collisional molecular dynamics in high-pressure gases. Our study demonstrates that rotational echoes enable the observation of extremely fast collisional dissipation, at timescales of the order of a few picoseconds, and possibly shorter. The decay of the rotational alignment echoes in CO_2 gas and CO_2-He mixture up to 50 bar was studied experimentally, delivering collision rates that are in good agreement with the theoretical expectations. The suggested measurement protocol may be used in other high-density media, and potentially in liquids.

The echo phenomenon is well known in various domains of physics, ranging from NMR spectroscopy [1,2] and nonlinear optics [3,4] to plasma physics [5,6] and physics of particle accelerators [7,8]. The effect relates to the impulsive stimulation of an ensemble of slightly nonidentical nonlinear objects (interacting or noninteracting). A single stimulus induces a coherent collective response signal that dies quickly due to the dispersion in the properties of individual objects (inhomogeneous broadening). The second stimulus, applied with a delay τ_{12}, results in a similar fast disappearing coherent response. However, if one continues observing the system for an additional time period of τ_{12}, the system produces another impulsive collective signal (echo) without any further stimulation. Moreover, in some cases, further echoes may be observed after waiting for more time ($2\tau_{12}$, $3\tau_{12}$, etc.). The echo is essentially a classical phenomenon that should be distinguished from the quantum revivals [9–12]. In addition to the fundamental importance of this generic effect, the echoes found multiple applications, mostly as a platform for measuring dephasing processes caused by irreversible dissipation. Recently, a new kind of echo was discovered in the rotational motion of molecules, the so-called rotational alignment echoes, including regular, high-order, and fractional echoes [13,14], rotated and imaginary echoes [15,16], and the echo-enabled rephasing of centrifugal distortions [17].

The present Letter describes the first study related to ultrafast collisional dissipation of rotational echoes generated in high-pressure molecular gases. The decay of the rotational revivals has been successfully used in the past to investigate the collisional dynamics in low-pressure gases [18,19]; however this approach becomes completely inefficient when the average time between collisions is comparable or shorter than the rotational revival time. As shown in this Letter, the rotational alignment echoes provide a powerful tool for studying collisional effects in dense gases and, potentially, in liquids.

Traditional echo spectroscopies like spin echo [1,2] and photon echo [3,4] disengage the homogeneous broadening from the overwhelming inhomogeneous broadening of investigated transitions by recording the corresponding echo response as a function of the delay between two excitation pulses. In these cases, the amplitude of the echoes is practically independent of the delay between the kicking stimuli (pulses) when the homogeneous broadening is negligible. Therefore, any decay of the echo amplitude directly reflects the irreversible dephasing.

The mechanism of the echoes in molecular alignment is quite different from the spin echo or photon echo, which makes them sensitive to both the pulse intensities, and to the delay τ_{12} [13]. Previous investigations of the rotational alignment echoes used rarified gases, and were focused on measuring the temporal and spatial evolution of echoes induced by two laser pulses ($\mathcal{P}_1$ and $\mathcal{P}_2$) separated by a delay τ_{12}. The experimental results clearly demonstrated strong dependence of the echo's amplitude on the intensity

of the second pulse, and on the delay τ_{12}. As shown in [13], for each τ_{12} there exists an optimal intensity of $\mathcal{P}_2$ that produces the strongest echo. A recent study [20] arrived at similar conclusions by studying the corresponding echo response in low-pressure OCS gas. This behavior is well explained by the classical analysis of rotational echoes based on the kick-induced filamentation of phase space of 2D rigid rotors [13,14].

In high-pressure gases, alignment echo spectroscopy requires developing a special measurement protocol for disentangling the collision-free dynamics of the echo amplitude from the effects of irreversible dissipation and dephasing in the molecular rotation dynamics. In order to define such a measurement strategy, we first conducted a series of simulations at collision-free conditions, by solving the Liouville–von Neumann equation for CO_2 molecules kicked by two nonresonant pulses through the anisotropic polarizability interaction. A temporal trace for the alignment metric ($\langle \cos^2(\theta) \rangle - 1/3$) [21] of CO_2 molecules (θ is the angle between the molecular axis and the direction of polarization of $\mathcal{P}_1$ and $\mathcal{P}_2$) is shown in Fig. 1(a), where the alignment responses induced around $\mathcal{P}_1$ and $\mathcal{P}_2$, the rotational echo (E) at $2\tau_{12}$, the second-order rotational echo (SE) at $3\tau_{12}$, and the quarter revival of the imaginary echo (IE) at $T_{\rm rev}/4 - \tau_{12}$ ($T_{\rm rev} = 42.7$ ps is the revival time of CO_2 molecules), are depicted with different colors. The strength of the rotational echo is characterized by the peak-to-dip amplitude as $\mathcal{S}_{\rm echo}$. It is clearly inferred from
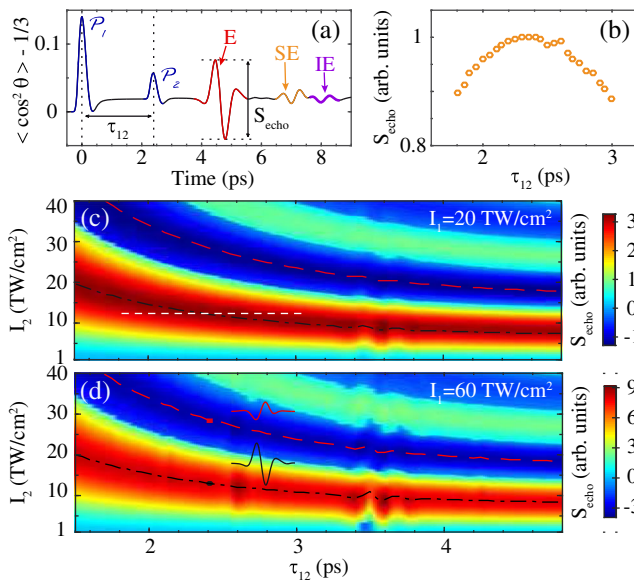
FIG. 1. (a) Temporal trace of the alignment signal of CO_2 kicked by two pump pulses ($\mathcal{P}_1$ and $\mathcal{P}_2$) in the collision-free conditions depicting the echo (E), the second-order echo (SE), and the imaginary echo (IE). (b) Variation of the echo amplitude along the horizontal dashed line depicted in (c). Calculated peak-to-dip amplitude of the rotational echo of CO_2, as a function of the delay τ_{12} and intensity of $\mathcal{P}_2$, as shown for two intensities of $\mathcal{P}_1$: $I_1 = 20$ TW/cm^2 (c) and $I_1 = 60$ TW/cm^2 (d).

Figs. 1(c)–1(d) that both the optimal intensity I_2 of $\mathcal{P}_2$ and optimal delay τ_{12} are well defined: the optimal I_2 can be found for each τ_{12} (consider a vertical straight cut of each contour plot) and similarly the optimal τ_{12} can be found for each I_2 (consider a horizontal straight cut of each contour plot). The black dot-dashed lines connect the optimal values of I_2 for varying τ_{12}, featuring that shorter delays necessitate higher $\mathcal{P}_2$ intensities to get the echo best rephased, and, alternatively, larger I_2 require shorter delays to maximize the echo. Therefore, one cannot simply find a unique optimal intensity for all the delays in rotational echoes, in sharp contrast, say, to photon echoes where the optimal strength of the second pulse always corresponds to a π pulse [4]. It is worth mentioning that the temporal profile of the rotational echo can be even reversed at higher than optimal intensities [represented by negative values plotted in Figs. 1(c)–1(d)], and the second optimal I_2 for the reversed echoes can be similarly defined (red dashed lines). Moreover, the dependence of rotational echoes on the intensity I_1 of $\mathcal{P}_1$ can be globally factorized out given the same shape of the contour plots obtained at two distinct values of I_1 shown in Figs. 1(c) and 1(d) with only the increment of color scales. This entangled dependence of rotational echoes on I_2 and τ_{12} is also well captured by the classical model of 2D rigid rotors [13], where the echo response is determined by the product of $I_2 \cdot \tau_{12} = \alpha$, where α is a constant independent of I_1. Finally, note that the maximal echo amplitudes, obtained by adjusting I_2 at each delay, are identical with less than 4% variations for the same I_1 inside the investigated range of τ_{12} (1.5–4.8 ps), except for a local "perturbation" occurring around $\tau_{12} \approx 3.6$ ps in Figs. 1(c) and 1(d) attributed to the imaginary echo [22].

Based on the numerical results discussed above, two strategies can be envisaged to utilize the rotational echoes to measure the ultrafast collisional dissipation of molecular rotors at high densities (high pressures), where quantum revivals of molecular alignment induced by a single pulse are hardly exploitable because of their long revival times [19]. The first one is to measure the maximum amplitudes of echoes generated at each delay τ_{12} by adaptive optimization of the corresponding intensity I_2 [20]. However, a systematic adjustment of intensity at different delays can introduce some experimental uncertainties, especially in high-density samples where the quickly damped amplitude of the echo signal tends to degrade the judicious control of the intensity. The other strategy is to find a compromised and fixed intensity I_2 for which the echo amplitude varies little over a limited range of τ_{12} retained for experiments. This is the strategy effectively employed in this work to interrogate the collisional decay of rotational echoes of CO_2 molecules, at high densities and/or diluted with high-pressure helium. The compromised intensity I_2 is found around 13 TW/cm^2, which renders the amplitudes of rotational echoes relatively uniform with less than 10%

variations, for delays τ_{12} scanned between 1.8 and 3.0 ps in collision-free conditions, as shown in Fig. 1(b).

The rotational echoes are measured by using a balanced detection of time-resolved birefringence of gas phase molecules impulsively aligned by two successive laser kicks. Details about the experimental setup are provided in the Supplemental Material [22]. Briefly, two collinear amplified 100 fs laser pulses with parallel linear polarizations, temporally separated by the adjustable delay τ_{12}, are tightly focused in a high-pressure static cell specially designed for polarization resolved high-pressure measurements. The transient birefringence resulting from the ultrafast anisotropic redistribution of molecule orientations is decoded by a probe pulse polarized at 45° with respect to $\mathcal{P}_1$ and $\mathcal{P}_2$. The probe beam is spatially overlapped with the two collinear pump beams in the focus, with a small crossing angle. The modification of the polarization of the probe pulse is analyzed with a highly sensitive balanced detector providing a heterodyne signal

$$S(\tau_{12}, \tau) \propto \int_{-\infty}^{\infty} I_3(t - \tau) \left[\langle\cos^2(\theta)\rangle(t, \tau_{12}) - \frac{1}{3} \right] dt, \quad (1)$$

where $\langle\cos^2(\theta)\rangle(t, \tau_{12})$ is the alignment metric as shown in Fig. 1(a) and I_3 is the probe intensity. The ultrafast dissipation of molecular alignment is inferred from the decay of the rotational echo observed by scanning the delay τ between the probe pulse and $\mathcal{P}_1$ for different fixed values of the delay τ_{12} between $\mathcal{P}_1$ and $\mathcal{P}_2$. Two molecular systems were investigated: pure CO_2 and CO_2-He mixture. These systems are of interest because of their well documented collisional decay rates from both experiment and theory (see, e.g., [18,19] and those cited in the discussion of line broadening data at the end of this Letter). Additionally, reliable intermolecular potentials, essential ingredients of the theoretical simulations (see below), are available for the involved collisional pairs. Regarding pure CO_2, it should be noted that the high peak powers required for the observation of the rotational echoes lead to nonlinear propagation effects for high gas densities, which are not observed for CO_2 diluted in He in the same density range, due to the much weaker nonlinear polarizability of He compared to CO_2 [29]. Considering the investigated pressure range and the tight-focusing geometry of the experiment, we observed that the propagation effects affect the intensity of $\mathcal{P}_2$ by ≈30% in the overlapping region of the three pulses. Since the amplitude of the echo is strongly dependent on the $\mathcal{P}_2$ intensity, the energy of $\mathcal{P}_2$ delivered by the laser was corrected by optimizing the peak-to-dip amplitude of the echo signal at $\tau_{12} = 2.4$ ps for each gas pressure so as to keep the intensity in the probe gas volume close to the compromised value. In contrast, the energy of $\mathcal{P}_1$ was not corrected as its intensity does not affect the τ_{12} dependence of the echo amplitude, as shown in Figs. 1(c) and 1(d). Finally, note that the plasma

contribution to the relaxation of the echo can be neglected, considering the very low relative density of the plasma, guaranteed by the intensities of $\mathcal{P}_1$ and $\mathcal{P}_2$ used in the experiment, as well as the small scattering cross sections for electron collisions with CO_2 [30].

In parallel with the experiments, theoretical calculations were also performed using classical molecular dynamics simulations (CMDS). These simulations, carried following Ref. [18], provide the time dependence of $\langle\cos^2(\theta)\rangle(t)$ for given values of I_1, I_2, τ_{12}, and gas density. They were performed, free of any adjustable parameters, as detailed in the Supplemental Material [22].

In a first step, the strategy introduced in Fig. 1 was tested experimentally. Typical results are presented in Fig. 2(a) where a series of temporal traces of molecular alignment is recorded for different delays τ_{12} and for an intensity I_2 set around 13 TW/cm². This value was found by optimizing the amplitude of the echo at $\tau_{12} = 2.4$ ps. These measurements were conducted at room temperature in pure CO_2 kept at low pressure in order to avoid any noticeable collisional decay of the echo signal within the investigated temporal range $\Delta\tau$. As a consequence, the slight change of the echo amplitude observed with respect to τ_{12} is mainly due to the inherent response of single molecules and also to the stability of the experiment. In agreement with the theoretical predictions of Fig. 1(b), the variation of the echo amplitudes over the investigated range of τ_{12} is less than 10%.
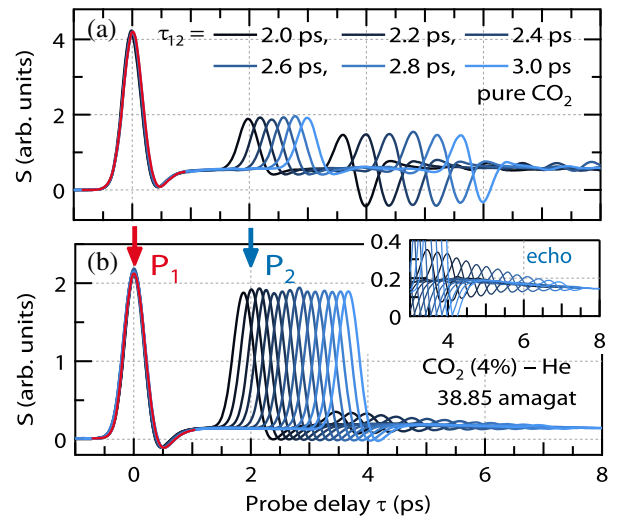
FIG. 2. (a) Low-pressure temporal traces of the echo recorded in CO_2 for different time delays τ_{12} between the pulse $\mathcal{P}_1$ and $\mathcal{P}_2$ as a function of the probe delay τ defined with respect to $\mathcal{P}_1$. The intensity of $\mathcal{P}_2$ is set to the optimal value for the delay $\tau_{12} = 2.4$ ps, i.e., 13 TW/cm² (see text). (b) High-pressure temporal traces in CO_2-He gas mixture at a pressure of 43.5 bar with an enlargement of the echo decay shown in the inset. The estimated intensity of $\mathcal{P}_1$ is 20 TW/cm². The positions of the alignment peaks respective to $\mathcal{P}_1$ and $\mathcal{P}_2$ are marked with arrows.

Next, echoes of CO_2 were recorded at the pressure of 43.5 bar in a CO_2-He mixture over a temporal probe window $\Delta\tau = 9$ ps, using the same strategy as in Fig. 2(a). Note that for such high pressure, the alignment revivals of CO_2 separated by $T_{rev}/4 \approx 10.7$ ps cannot be properly used anymore for tracking collisional processes [19,31]. As shown in Fig. 2(b), the collisional dissipation of the echo is evidenced by varying the delay τ_{12}. The corresponding peak-to-dip echo amplitudes are plotted in Fig. 3(a). We apply to the data an exponential least-squares fit $\exp(-2\tau_{12}\gamma)$, where γ defines the relaxation rate of the echo estimated at a given density. As can be seen, the agreement between CMDS-predicted and measured results is excellent in this particular case.

In order to assess the consistency of our measurements, we report in Fig. 3(b) the collisional decay rate γ of the echo

(a)

(b)

(c)
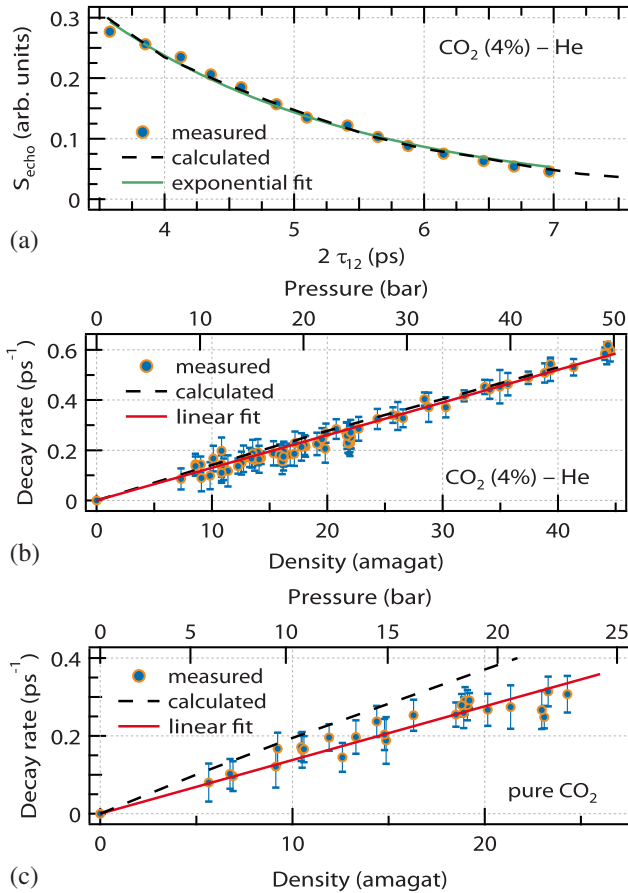
FIG. 3. (a) Peak-to-dip amplitude of the echo (filled circles) recorded in a CO_2-He gas mixture ($P = 43.5$ bar) as a function of τ_{12} compared with the CMDS simulations (dashed line). Least-squares fitting of the experimental data with an exponential law (solid line). (b) Decay rates γ of the echo (filled circles) measured for various density of the gas mixture with the linear fit (solid line) of the data and the CMDS calculations (dashed line). The error bars reflect the dispersion of the measurements. The bottom (top) x axis denotes the gas density (pressure) in units of amagat (bar). (c) Decay rates γ measured in pure CO_2.

determined for different gas densities of the mixture (expressed hereafter in amagat units) corresponding to pressures ranging from 8 to 50 bar. Keep in mind that in the binary collision regime, which is valid in this pressure range, the collisional relaxation rate of the alignment signal should be proportional to the number density. We can see from the linear fit of the data that this is well verified for the measured echoes as is also evidenced by the results of the CMDS model presented on the same figure. The experimental value of the decay time constant of the echo $\tau_E = \gamma_0^{-1}$, with γ_0 the slope versus density extracted from the linear least-squares fitting of the data, is reported in Table I together with the value predicted by the CMDS model. As shown, the experimental observation ($\tau_E = 77$ ps amagat) is well reproduced by the theory ($\tau_E = 74$ ps amagat). For comparison, we also provide in the same table the decay time constant of the alignment revivals of CO_2 ($\tau_R = 83$ ps amagat) measured at lower pressure in the same gas mixture by investigating the field-free alignment signal with a standard (two pulses) pump-probe technique [19]. The good match between the experimental values, that are both well reproduced by the CMDS model, reveals that the decay rates of the revival and echo are comparable for the CO_2-He collisions. In order to figure out if this finding applies to other high-pressure gases, we performed measurements of rotational echoes in pure CO_2 for which the decay rate of the alignment revivals have also been measured [19] and computed [18]. The corresponding decay rate of the echoes is presented in Fig. 3(c) together with the CMDS simulations. The data summarized in Table I show that the dissipation of the echo and alignment revivals in pure CO_2 occurs with a comparable time constant, which is consistent with the results obtained in the gas mixture. However, note that the CMDS reproduce more closely the experimental value in CO_2-He than in pure CO_2, which was already observed in probing the dissipation of molecular alignment revivals [18,19]. It is worth noting that, for CO_2, the decay rates of the echo τ_E and of the alignment revivals τ_R are close to that associated to the dissipation of the dipole autocorrelation function [32], τ_D [as can be obtained through $\tau_D = (2\pi c \langle\gamma_B\rangle)^{-1}$, where γ_B is the average pressure broadening coefficient in cm^{-1}/amagat in the spectral domain]. Indeed, experiments yield $\tau_D = 51.2$ ps amagat for pure CO_2 [33] and 82.3 ps

TABLE I. Measured and calculated collisional decay time constants τ_E and τ_R in picosecond amagat units for infinitely diluted CO_2-He gas mixture and pure CO_2 gas. The numbers in parenthesis correspond to three standard deviations.

	CO_2-He		CO_2	
	Echo	Revivals	Echo	Revivals
Experiment	77(4)	83(8) [19]	73(7)	68(7) [19]
CMDS model	74(7)	81 [18]	53(2)	57 [18]

amagat for CO_2-He [34,35], while direct calculations lead to very close values of 51.3 ps amagat [32] and 79.6 ps amagat [35], respectively. The finding that $\tau_E \approx \tau_R \approx \tau_D$ for CO_2 and CO_2-He is in apparent disagreement with the recently measured value $\tau_E = 13$ ps amagat for pure OCS gas [20], about 2.5 times smaller than the experimental values $\tau_R = 32.4$ ps amagat [36] and $\tau_D = 31.4$ ps amagat [37,38]. We have no explanation for this difference that is not reproduced by direct calculations [22], which lead to $\tau_E = 45$ ps amagat, $\tau_R = 36.0$ ps amagat. The dissipation of the echoes and revivals both result from collision-induced changes of the molecular rotational speeds. The associated decay time constants are expected to be of the same order, as confirmed by the present results. However, differences may arise, depending on the collisional pairs, due to the different nature (classical and quantum) of these two alignment signatures.

The present Letter shows that rotational alignment echoes represent a unique method for probing ultrafast rotational relaxation for elevated molecular densities in systems for which "usual" alignment revivals cannot be observed anymore. A first natural and tempting extension of the present study would thus be to carry similar investigations in the liquid phase for which any rotational information or coherence imprinted in the system has vanished due to very quick thermalization at timescales of a few ps. In principle, femtosecond timescales should be accessible by reducing the duration of the laser pulses. Similarly, it would be very interesting to apply rotational echoes to molecules embedded in helium nanodroplets. For instance, collective rotation of the iodine molecule and its solvation shell can lead to field-free molecular alignment revivals [39]. Very recently, it has been demonstrated that 1D or 3D alignment of large and complex molecules inside helium nanodroplets could persist for several tens of picoseconds after the rapid truncation of a strong laser pulse [40]. Echoes could therefore provide a mean for real-time studies of nonequilibrium solute-solvent ultrafast dynamics.

*olivier.faucher@u-bourgogne.fr
†jwu@phy.ecnu.edu.cn
‡ilya.averbukh@weizmann.ac.il

[1] E. L. Hahn, Phys. Rev. **80**, 580 (1950).
[2] E. L. Hahn, Phys. Today **6**, No. 11, 4 (1953).
[3] N. A. Kurnit, I. D. Abella, and S. R. Hartmann, Phys. Rev. Lett. **13**, 567 (1964).
[4] I. D. Abella, N. A. Kurnit, and S. R. Hartmann, Phys. Rev. **141**, 391 (1966).
[5] R. M. Hill and D. E. Kaplan, Phys. Rev. Lett. **14**, 1062 (1965).
[6] R. W. Gould, T. M. O'Neil, and J. H. Malmberg, Phys. Rev. Lett. **19**, 219 (1967).
[7] G. Stupakov, Echo effect in hadron colliders, SSC Report No. SSCL-579, 1992.
[8] G. Stupakov and S. Kauffmann, Superconducting Supercollider Laboratory Report No. SSCL-587, 1992.
[9] J. H. Eberly, N. B. Narozhny, and J. J. Sanchez-Mondragon, Phys. Rev. Lett. **44**, 1323 (1980).
[10] J. Parker and C. R. Stroud, Phys. Rev. Lett. **56**, 716 (1986).
[11] I. S. Averbukh and N. Perelman, Phys. Lett. A **139**, 449 (1989).
[12] R. Robinett, Phys. Rep. **392**, 1 (2004).
[13] G. Karras, E. Hertz, F. Billard, B. Lavorel, J. M. Hartmann, O. Faucher, E. Gershnabel, Y. Prior, and I. S. Averbukh, Phys. Rev. Lett. **114**, 153601 (2015).
[14] G. Karras, E. Hertz, F. Billard, B. Lavorel, G. Siour, J. M. Hartmann, O. Faucher, E. Gershnabel, Y. Prior, and I. S. Averbukh, Phys. Rev. A **94**, 033404 (2016).
[15] K. Lin, P. Lu, J. Ma, X. Gong, Q. Song, Q. Ji, W. Zhang, H. Zeng, J. Wu, G. Karras et al., Phys. Rev. X **6**, 041056 (2016).
[16] K. Lin, J. Ma, X. Gong, Q. Song, Q. Ji, W. Zhang, H. Li, P. Lu, H. Li, H. Zeng et al., Opt. Express **25**, 24917 (2017).
[17] D. Rosenberg, R. Damari, S. Kallush, and S. Fleischer, J. Phys. Chem. Lett. **8**, 5128 (2017).
[18] J.-M. Hartmann, C. Boulet, T. Vieillard, F. Chaussard, F. Billard, O. Faucher, and B. Lavorel, J. Chem. Phys. **139**, 024306 (2013).
[19] T. Vieillard, F. Chaussard, F. Billard, D. Sugny, O. Faucher, S. Ivanov, J. M. Hartmann, C. Boulet, and B. Lavorel, Phys. Rev. A **87**, 023409 (2013).
[20] D. Rosenberg, R. Damari, and S. Fleischer, Phys. Rev. Lett. **121**, 234101 (2018).
[21] H. Stapelfeldt and T. Seideman, Rev. Mod. Phys. **75**, 543 (2003).
[22] See Supplemental Material at http://link.aps.org/supplemental/10.1103/PhysRevLett.122.193401 for details about the experimental setup, the interplay between echoes and imaginary echoes, and the CMDS model, which includes Refs. [23–28].
[23] V. Renard, M. Renard, S. Guérin, Y. T. Pashayan, B. Lavorel, O. Faucher, and H. R. Jauslin, Phys. Rev. Lett. **90**, 153601 (2003).
[24] J. M. Hartmann and C. Boulet, J. Chem. Phys. **136**, 184302 (2012).
[25] S. Bock, E. Bich, and E. Vogel, Chem. Phys. **257**, 147 (2000).

[26] M. Jeziorska, W. Cencek, K. Patkowski, B. Jeziorski, and K. Szalewicz, J. Chem. Phys. **127**, 124303 (2007).

[27] T. Korona, R. Moszynski, F. Thibault, J.-M. Launay, B. Bussery-Honvault, J. Boissoles, and P. E. S. Wormer, J. Chem. Phys. **115**, 3074 (2001).

[28] J. P. Bouanich and G. Blanquet, J. Quant. Spectrosc. Radiat. Transfer **40**, 205 (1988).

[29] D. P. Shelton, Phys. Rev. A **42**, 2578 (1990).

[30] Y. Itikawa, J. Phys. Chem. Ref. Data **31**, 749 (2002).

[31] S. Ramakrishna and T. Seideman, Phys. Rev. Lett. **95**, 113001 (2005).

[32] J. M. Hartmann, H. Tran, N. H. Ngo, X. Landsheere, P. Chelin, Y. Lu, A. W. Liu, S. M. Hu, L. Gianfrani, G. Casa *et al.*, Phys. Rev. A **87**, 013403 (2013).

[33] A. Predoi-Cross, A. V. Unni, W. Liu, I. Schofield, C. Holladay, A. R. W. McKellar, and D. Hurtmans, J. Mol. Spectrosc. **245**, 34 (2007).

[34] F. Thibault, J. Boissoles, R. Le Doucen, J. P. Bouanich, P. Arcas, and C. Boulet, J. Chem. Phys. **96**, 4945 (1992).

[35] F. Thibault, B. Calil, J. Boissoles, and J. M. Launay, Phys. Chem. Chem. Phys. **2**, 5404 (2000).

[36] R. Damari, D. Rosenberg, and S. Fleischer, Phys. Rev. Lett. **119**, 033002 (2017).

[37] S. Matton, F. Rohart, R. Bocquet, G. Mouret, D. Bigourd, A. Cuisset, and F. Hindle, J. Mol. Spectrosc. **239**, 182 (2006).

[38] M. A. Koshelev, M. Y. Tretyakov, F. Rohart, and J.-P. Bouanich, J. Chem. Phys. **136**, 124316 (2012).

[39] B. Shepperson, A. A. Sondergaard, L. Christiansen, J. Kaczmarczyk, R. E. Zillich, M. Lemeshko, and H. Stapelfeldt, Phys. Rev. Lett. **118**, 203203 (2017).

[40] A. S. Chatterley, C. Schouder, L. Christiansen, B. Shepperson, M. H. Rasmussen, and H. Stapelfeldt, Nat. Commun. **10**, 133 (2019).

Correction: The previously published Fig. 3(c) contained scaling errors and has been fixed.